

## Scale-up of tubular photobioreactors

E. Molina Grima<sup>1\*</sup>, F.G. Ación Fernández<sup>1</sup>, F. García Camacho<sup>1</sup>, F. Camacho Rubio<sup>2</sup> & Y. Chisti<sup>1</sup>

<sup>1</sup> *Department of Chemical Engineering, University of Almería, E-04071 Almería, Spain*

<sup>2</sup> *Department of Chemical Engineering, University of Granada, E-18071 Granada, Spain*

(\* Author for correspondence)

Received 1999; revised 4 April 2000; accepted 6 April 2000

*Key words*: light/dark cycles, microalgae, *Phaeodactylum tricorutum*, photobioreactors, scale-up

### Abstract

The effect of the light/dark cycle frequency on the productivity of algal culture at different day-averaged irradiance conditions was evaluated for *Phaeodactylum tricorutum* grown in outdoor tubular photobioreactors. The photobioreactor scale-up problem was analyzed by establishing the frequency of light–dark cycling of cells and ensuring that the cycle frequency remained unchanged on scale-up. The hydrodynamics and geometry related factors were identified for assuring an unchanged light/dark cycle. The light/dark cycle time in two different tubular photobioreactors was shown to be identical when the linear culture velocity in the large scale device ( $U_{LL}$ ) and that in the small scale unit ( $U_{LS}$ ) were related as follows:

$$U_{LL} = \frac{f^{9/7}}{\alpha^{8/7}} U_{LS}.$$

Here  $f$  is the scale factor (i.e., the ratio of large-to-small tube diameters),  $\alpha$  is a function of the illuminated volumes in the two reactors, and ‘dark’ refers to any zone of the reactor where the light intensity is less than the saturation value. The above equation was tested in continuous cultures of *P. tricorutum* in reactors with 0.03 m and 0.06 m diameter tubes, and over the workable culture velocity range of 0.23 to 0.50 m s<sup>-1</sup>. The predicted maximum realistic photobioreactor tube diameter was about 0.10 m for assuring a culture performance identical to that in reactors with smaller tubes.

### List of abbreviations

$a$	Parameter in Equation (22) (g L <sup>-1</sup> d <sup>-1</sup> )	$g$	Gravitational acceleration (m s <sup>-2</sup> )
$b$	Parameter in Equation (22) (g m <sup>2</sup> s μE <sup>-1</sup> d <sup>-1</sup> )	$I_s$	Saturating light intensity (μE m <sup>-2</sup> s <sup>-1</sup> )
$C_b$	Biomass concentration (g L <sup>-1</sup> )	$I_w$	Instantaneous photon-flux of PAR on reactor’s surface (μE m <sup>-2</sup> s <sup>-1</sup> )
$C_f$	Fanning friction factor (–)	$I_{wm}$	Day-averaged irradiance (μE m <sup>-2</sup> s <sup>-1</sup> )
$c$	Parameter in Equation (23) (s <sup>-1</sup> )	$K_a$	Culture absorption coefficient (m <sup>2</sup> kg <sup>-1</sup> )
$D$	Dilution rate (h <sup>-1</sup> )	$K_v$	Frequency for half the maximum productivity (Hz)
$d$	Parameter in Equation (23) (m <sup>2</sup> μE <sup>-1</sup> )	$l_{\text{eddies}}$	Length of microeddies (m)
$d_l$	Depth of the light zone (m)	$OD_{xxx}$	Optical density at xxx nm wavelength (–)
$d_t$	Tube diameter (m)	PAR	Photosynthetically active radiation
$d_{tL}$	Tube diameter at the larger scale (m)	$P_b$	Biomass productivity based on 10 h daylight period (g L <sup>-1</sup> d <sup>-1</sup> )
$d_{tS}$	Tube diameter at small scale (m)		
$f$	Scale factor (–)		

$P_{b\max}$	Maximum biomass productivity based on 10 h daylight period ( $\text{g L}^{-1} \text{d}^{-1}$ )
$Q_R$	Volumetric rate of fluid interchange per unit tube length ( $\text{m}^2 \text{s}^{-1}$ )
Re	Reynolds number (—)
$s$	Length of arc in Figure 1 (m)
$t_c$	Cycling time (s)
$t_{cL}$	Cycling time at large scale (s)
$t_{cS}$	Cycling time at small scale (s)
$t_d$	Time spent in the dark zone (s)
$t_f$	Time spent in the photic zone (s)
$U_L$	Superficial liquid velocity ( $\text{m s}^{-1}$ )
$U_{LL}$	Superficial liquid velocity at large scale ( $\text{m s}^{-1}$ )
$U_{LS}$	Superficial liquid velocity at small scale ( $\text{m s}^{-1}$ )
$U_R$	Radial velocity ( $\text{m s}^{-1}$ )
$U_{RL}$	Radial velocity at large scale ( $\text{m s}^{-1}$ )
$U_{RS}$	Radial velocity at small scale ( $\text{m s}^{-1}$ )
$V_f$	Volume of light zone ( $\text{m}^3$ )
$V_d$	Dark volume ( $\text{m}^3$ )
$X_p$	Total pigment content in biomass ( $\text{mg g}^{-1}$ )

### Greek symbols

$\alpha$	Factor dependent on the illuminated volume fraction (Equation 8) (—)
$\theta$	Defining angle (rads)
$\Gamma$	Light integration function (—)
$\Gamma_{\max}$	Maximum value of $\Gamma$ (—)
$\mu$	Viscosity of the culture broth (Pa s)
$\nu$	Light/dark cycle frequency (Hz)
$\xi$	Energy dissipation per unit mass ( $\text{W kg}^{-1}$ )
$\rho$	Density of the fluid ( $\text{kg m}^{-3}$ )
$\tau_o$	Wall shear stress ( $\text{N m}^{-2}$ )
$\phi$	Illuminated volume fraction of the reactor (photic volume fraction) (—)

### Introduction

Tubular photobioreactors consist of straight, coiled or looped transparent tubing arranged in various ways

for maximizing sunlight capture. Phototrophic cultures are circulated through the tubes by various methods; use of airlift circulators is especially common. Properly designed tubular photobioreactors completely isolate the culture from potentially contaminating external environments, hence, allowing extended duration monoalgal culture. Scale-up of tubular photobioreactors by increasing the diameter of tubes is practicable only within narrow limits. How such scale-up should be engineered is not clear, although essential principles of an approach to scale-up have been enunciated (Molina Grima et al., 1999). At sufficiently high biomass concentrations, the reactor volume can be demarcated into a photic zone and a 'dark' zone. In the photic zone, the light intensity is such that it does not limit growth or photosynthesis. In the dark zone, the light intensity may range from zero to just below the saturation light intensity. Because of turbulence, the cells in a dense culture fluid flowing through the tubes continually move between light and dark zones. Consequently, the cells experience light/dark cycling. In a given tube, the cycle frequency depends on the relative volume of the photic zone (influenced by the external irradiance, the tube diameter, the biomass concentration and pigmentation) and the intensity of turbulence (influenced mainly by the velocity of flow).

The frequency of the light/dark cycle is known to affect productivity (e.g. Kok, 1953; Phillipps & Myers, 1954; Grobbelaar, 1994; Grobbelaar et al., 1996; Matthijs et al., 1996; Nedbal et al., 1996; Merchuk et al., 1998; Janssen et al., 1999). The productivity increases hyperbolically with increasing frequency of the light/dark cycle. The highest photosynthetic efficiency is generally obtained when the flash cycle frequency becomes identical to the turnover rate of electrons in the photosystem II of the photosynthetic apparatus (Kroon, 1994). According to a recently published scale-up criterion, the maximum duration of the dark time between adjacent light periods must remain below a critical value, that, if exceeded, would cause a decline in the rate of photosynthesis and the culture productivity (Molina Grima et al., 1999). The critical length of dark period appears to be culture specific and can be determined by subjecting the cells to different cycle frequencies until a decline in productivity is detected (Terry, 1986; Grobbelaar, 1994; Merchuk et al., 1998; Janssen et al., 1999). The optimal light/dark cycle frequency also depends on the light intensity in the photic period, as reported for *Phaeodactylum tricornutum* (Terry, 1986).

Earlier studies of the light/dark cycling effects generally used cultures so dilute that during the flash period the cells were subjected to a uniform light intensity. Flash periods were interspersed with periods of total darkness. Unfortunately, the situation in practical photobioreactors with dense cultures is quite different from the idealized light/dark cycling scenario used in the past. In most practical cases, the cells move randomly with the flow from a photic zone to light limited zones. The light intensity never cycles sharply from total darkness to homogeneous light; instead, there is a continuum change in the light intensity from the photic to the light limited levels. In some cases, the reactor may also have regions in which the light level declines to less than the compensation threshold. As a consequence of this gradual change in the light level, the light/dark cycle data measured in the past are not directly relevant to interpreting the performance of practical photobioreactors. For the purpose of analysis of these reactors, light and dark zones need to be defined differently than in the past.

This paper develops a method for relating the light/dark frequency to prevailing hydrodynamics and irradiance level in a photobioreactor. The light zone is defined as that in which the light intensity is at saturation value, or greater. The dark zone is one where the light intensity is below the saturation threshold. Dependence of culture productivity on cycle frequency is documented. Scale-up capability is proved using the criterion of keeping constant the light/dark cycle frequency in reactors of different diameters. Biomass productivity is influenced by four major variables—tube diameter,  $d_t$ ; culture flow velocity  $U_L$ ; the sunlight intensity received by the culture,  $I_{wm}$ ; and the dilution rate,  $D$ . Of these, the first two influence the cycling frequency most strongly.

### Scale-up criterion

As previously noted (Molina Grima et al., 1999), two geometrically similar tubular photobioreactors operating at identical residence times should have identical productivities so long as their light/dark cycling times (or inverse of cycling times, i.e. cycling frequencies) are the same. To quantify the light/dark cycling time in a tube of a given diameter, we need to know the relative volumes of the light and dark zones and the velocity of fluid interchange between the zones. In an outdoor reactor, the relative volumes of dark and photic zones are determined by factors such as the

season and time of day, that influence the position of the Sun with respect to the photobioreactor. For any tube of diameter  $d_t$ , the light distribution inside the tube can be estimated using an earlier published irradiance model (Acién Fernández et al., 1997) that has been experimentally validated for different algae and reactors (García Camacho et al., 1999). Using such a model, the light profile within a tube may be computed as shown in Figure 1 for two horizontal tubular reactors of different tube diameters on days with similar irradiance levels and biomass concentrations.

In a reactor placed outdoors, the depth of the light zone  $d_l$  varies during the day as the Sun changes position. Using the profiles in Figure 1a, the proportion of the reactor volume with irradiance levels greater than the saturating light intensity ( $I_s$ ) may be obtained. At saturating light intensities the culture is no longer photolimited. The  $I_s$  value is species dependent and must be determined experimentally. In Figure 1, the dark volume  $V_d$  of the reactor where the irradiance level is lower than  $I_s$ , is calculated as the shaded area (Figure 1b) multiplied by the length of the tube. The interfacial area between the dark and light zones (Figure 1) equals the length of the boundary arc between the two zones (Figure 1b) multiplied by the tube length. The length of the boundary arc is estimated as follows: the shaded area in Figure 1a is approximated as the area of overlap of two circles having the same diameter as the photobioreactor tube (Figure 1b). The angle  $\theta$  (Figure 1b) specifies a circular segment with an area equal to half the area of the overlap zone and the length  $s$  of the boundary arc equals  $\theta d_t/2$ . If  $t_d$  is the maximum acceptable duration of the dark period between successive light periods, then the maximum residence time of fluid in the dark zone should be  $\leq t_d$  (Molina Grima et al., 1999). Therefore, the volumetric rate of fluid movement out of the dark zone is,

$$Q_R = \frac{\text{dark zone volume}}{t_d} = \frac{d_t^2(\theta - \sin \theta)}{2t_d}. \quad (1)$$

This  $Q_R$  value is on a unit tube length basis. The dark zone defining angle  $\theta$  is shown in Figure 1. Because all the fluid moving out of the dark zone must pass through the boundary between the light and the dark zones (Molina Grima et al., 1999), a fluid interchange velocity can be defined as follows:

$$U_R = \frac{Q_R}{s} = \frac{d_t(\theta - \sin \theta)}{2t_d \sin \theta} \quad (2)$$

and

$$t_d = \frac{d_t(\theta - \sin \theta)}{2U_R \sin \theta}. \quad (3)$$

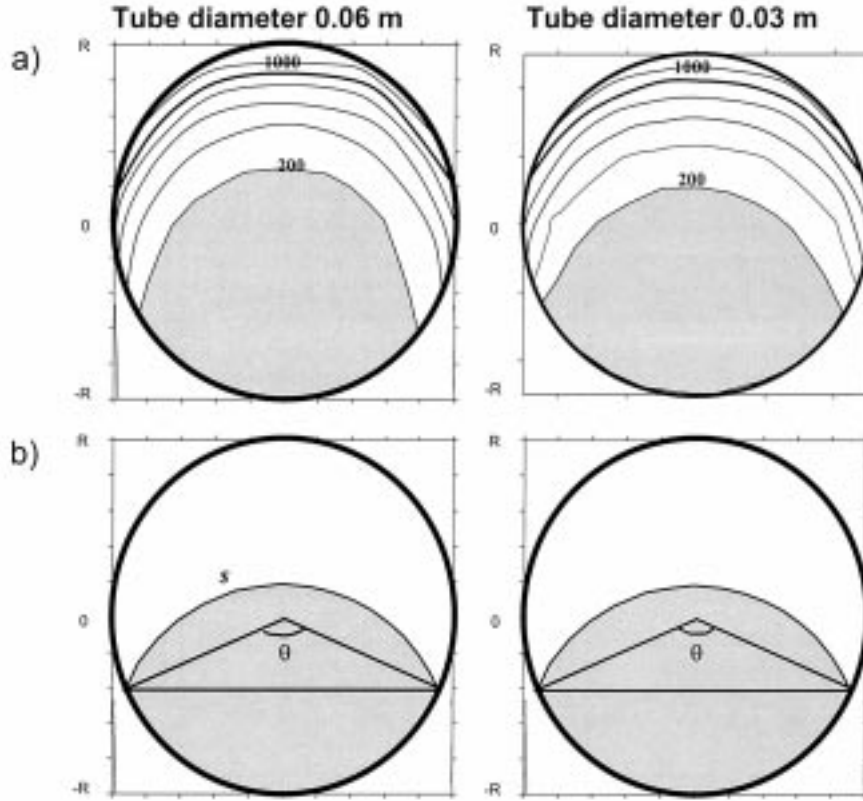


Figure 1. a) Computed light profiles ( $\mu\text{E m}^{-2} \text{s}^{-1}$ ) inside the tubes at midday for two different tube diameter at a dilution rate of  $0.040 \text{ h}^{-1}$ . The profiles were calculated using a previously published irradiance model (Acién Fernández et al., 1997). b) Simplified light profiles.

To ensure identical performance at the two scales, the light/dark cycling time  $t_c$ , i.e. the sum of the time spent by the cells in the photic and the dark zones at the two scales should be held constant. That is,  $t_c = t_f + t_d$  should be constant, where  $t_f$  and  $t_d$  are the times in the photic and the dark zones, respectively. Thus, for scale-up,

$$t_{cL} = t_{cS} \quad (4)$$

where  $t_{cL}$  and  $t_{cS}$  are the cycle times at large and small scales, respectively.

The light ( $t_f$ ) and dark periods ( $t_d$ ) are determined by the cycle frequency,  $\nu$ , which is equal to  $1/(t_f + t_d)$ . As previously noted, for a known level of external irradiance, biomass concentration, and absorption coefficient of the biomass, the fractional culture volume  $\phi$  that is illuminated (i.e. the photic volume fraction) can be estimated from the light profiles;  $\phi = V_f/(V_f + V_d)$ . If we assume that the volume

$V_f$  is proportional to the flash period  $t_f$ , and the dark volume  $V_d$  is proportional to the dark period  $t_d$ , the cycling time  $t_c$  can be expressed in terms of  $\phi$ , as follows:

$$t_c = t_d \left( \frac{1}{1 - \phi} \right). \quad (5)$$

Thus, the frequency  $\nu$  is:

$$\nu = \frac{1 - \phi}{t_d}. \quad (6)$$

According to the scale-up criterion, the frequency at two scales should be equal, or

$$\left( \frac{1 - \phi}{t_d} \right)_L = \left( \frac{1 - \phi}{t_d} \right)_S, \quad (7)$$

and, therefore,

$$t_{dL} = \left( \frac{1 - \phi_L}{1 - \phi_S} \right) t_{dS} = \alpha t_{dS} \quad (8)$$

where the subscripts  $S$  and  $L$  refer to small and large scales, respectively. Substitution of Equation (3) in Equation (8), produces the equation:

$$\left(\frac{d_t(\theta - \sin \theta)}{2U_R\theta}\right)_L = \left(\frac{1-\phi_L}{1-\phi_S}\right)\left(\frac{d_t(\theta - \sin \theta)}{2U_R\theta}\right)_S \quad (9)$$

As shown later, for otherwise identical conditions, the defining angle  $\theta$  is virtually identical at two scales. Simplification of Equation (9) provides the scale-up criterion, as follows:

$$\frac{d_{tL}U_{RS}}{\alpha d_{tS}U_{RL}} = 1. \quad (10)$$

If the scale factor is  $f$ , i.e.  $d_{tL} = f \cdot d_{tS}$ , then for identical performance, the large scale light-dark interchange velocity should be:

$$U_{RL} = \frac{f}{\alpha} U_{RS} \quad (11)$$

where  $f > 1$ .

Cells move radially with the fluid because of momentum transport between the turbulent core and the more quiescent boundary layer adjacent to walls. Thus, the radial velocity may be approximated as the characteristic velocity of turbulence in the center of the tube. The latter characteristic velocity (Davies, 1972) is given as:

$$U_R = \sqrt{\frac{\tau_o}{\rho}} \quad (12)$$

where  $\rho$  is the density of the fluid and  $\tau_o$  is the wall shear stress, calculated as:

$$\tau_o = \frac{1}{2} C_f \rho U_L^2. \quad (13)$$

In Equation (13),  $C_f$  is the Fanning friction factor that depends on Reynolds number (Re) in accordance with Blasius equation:

$$C_f \approx 0.08 \text{Re}^{-0.25}. \quad (14)$$

Substitution of Equation (14) and Equation (13) in Equation (12) leads to:

$$U_R = 0.2U_L \text{Re}^{-1/8} = \frac{1}{2} \sqrt{\frac{\xi d_t}{U_L}} \quad (15)$$

where  $\xi$ , the energy dissipation per unit mass, is calculated as follows:

$$\xi = \frac{2C_f U_L^3}{d_t}. \quad (16)$$

Thus, Equation (12) may be written as:

$$U_R = 0.2 \left(\frac{U_L^7 \mu}{d_t \rho}\right)^{1/8} \quad (17)$$

which allows the calculation of the radial velocity ( $U_R$ ) in the turbulent core as a function of the superficial liquid velocity ( $U_L$ ), the tube diameter ( $d_t$ ), and the density ( $\rho$ ) and viscosity ( $\mu$ ) of the culture broth. Using Equation (17) the scale-up criterion becomes:

$$U_{LL} = \frac{f^{9/7}}{\alpha^{8/7}} U_{LS}. \quad (18)$$

Equation (18) may be used to calculate the requisite liquid velocity in a large scale photobioreactor to satisfy the scale-up criterion. As pointed out later in this paper, the liquid velocity cannot increase without limit and a maximum allowable  $U_{LL}$  value restricts the maximum tube diameter  $d_{tL}$  at the larger scale.

## Materials and methods

### Organism and culture medium

The microalga used, *Phaeodactylum tricoratum* UTEX 640, was obtained from the culture collection of the University of Texas, Austin. This is a freshwater strain, but it tolerates a high salinity (Yongmanitchai & Ward, 1991). The inoculum for the photobioreactors was grown indoors under artificial light (230  $\mu\text{E m}^{-2} \text{s}^{-1}$  flux at the vessel's surface) using Mann and Myers' medium (1968). The culture temperature was 20 °C.

### Outdoor culture system

Two outdoor placed photobioreactors were used. The reactors consisted of a continuous run tubular loop solar receiver in which the culture fluid was circulated by an airlift device. The tube external diameters were 0.06 m and 0.03 m corresponding to internal diameters of 0.053 m and 0.025 m. The respective reactor volumes were 0.22 and 0.05  $\text{m}^3$ . A third reactor, also with a 0.06 m diameter (0.053 m internal diameter) tubular loop and a volume of 0.20  $\text{m}^3$  was also used and it differed from the others in the arrangement of the solar receiver (continuous run tubing arranged to occupy a more compact land area), but this difference was not substantial with respect to the other reactor with the same tube diameter (Ación Fernández, Fernández Sevilla, Sánchez Pérez, Molina Grima & Chisti, unpublished data). The dimensions and schematics of the reactors have been published previously

(Acién Fernández et al., 1998). The photobioreactors were made of Plexiglas. In all cases, the solar receiver loop was submerged in a pond of water held at  $20 \pm 2$  °C. The reactors were located in Almería, Spain ( $36^{\circ}50'$  N,  $2^{\circ}27'$  W).

#### Operating mode

The three photobioreactors were operated as continuous cultures at various dilution rates: 0.025, 0.040 and  $0.050 \text{ h}^{-1}$ . Fresh medium was added at a constant rate during 10-h daylight periods until the biomass concentration at sunrise was the same for four consecutive days, corresponding to attainment of a pseudo-steady state. In outdoor culture, the medium was Mann & Myers (1968), with nutrient concentrations tripled to avoid limitations. The dilution rate was interrupted during the night to prevent culture washout. The pH was controlled at 7.7 by injecting pure carbon dioxide as needed.

#### Solar irradiance

The instantaneous photon-flux density of photosynthetically active radiation (PAR) on the reactor's surface ( $I_w$ ) was measured periodically at different solar hours each day using a quantum scalar irradiance sensor (QSL 100, Biospherical Instruments Inc., San Diego, CA, U.S.A.). The instantaneous values were numerically integrated to obtain the day-averaged PAR,  $I_{wm}$ . The light profiles within the culture were estimated using the irradiance model of Acién Fernández et al. (1997), measured biomass concentration, and the culture absorption coefficient  $K_a$ . The culture biomass absorption coefficient depended on the total pigment content  $X_p$  in the biomass (Molina Grima et al., 1996), in accordance with the equation:

$$K_a = 0.0105 + 0.0299X_p. \quad (19)$$

The irradiance profiles inside tubes could be used to demarcate the cross-section of the solar receiver tubes into a 'dark' zone with irradiance values below saturation, or  $\sim 185 \mu\text{E m}^{-2} \text{ s}^{-1}$  (Mann & Myers, 1968; Acién Fernández et al., 1998), the remainder being the photic zone.

#### Analytical methods

The biomass concentration was estimated hourly during daylight from the measured optical density (OD) of the culture. The optical density was measured spectrophotometrically (Hitachi U-1000) at 625 nm

wavelength in a cuvette with 1-cm light path. The relationship between the biomass concentration and the optical density (OD) was:

$$C_b(\text{g} \cdot \text{L}^{-1}) = 0.38 \cdot \text{OD}_{625} \quad (20)$$

where  $C_b$  is the biomass concentration. The spectrophotometric determination of biomass was periodically verified by dry weight measurements on samples which had been centrifuged ( $1800 \times g$ ), washed with 0.5 M HCl and distilled water to remove non-biological adhering materials such as mineral precipitates, and freeze-dried. In order to determine the pigment content of the biomass, the cultures were sampled early in the morning each day after a quasi-steady-state had been attained. The chlorophyll content was measured according to the method of Hansmann (1973). Carotenoid determination was according to Whyte (1987).

## Results and discussion

Productivity data of 42 outdoor continuous culture experiments are summarized in Tables 1 and 2. The data are sorted into two groups according to tube diameter,  $d_t$ . The values for the radial velocity  $U_R$ , the angle  $\theta$ , the times  $t_d$  and  $t_c$ , and the frequency  $\nu$  were obtained using the various equations noted in an earlier section of this paper. Note in particular (Tables 1 and 2) that for days with similar levels of irradiance and dilution rates, the angle  $\theta$  is almost the same for the two tubes. For example, experiments 2 to 6 and 22 to 28, performed at a dilution rate of  $0.025 \text{ h}^{-1}$  and similar day-averaged irradiances, provided a  $\theta$  value of about 2.9 radians. Again,  $\theta$  values were similar (Tables 1 and 2) for experiments 7 to 11 and 29 to 34, performed at dilution rates of  $0.04 \text{ h}^{-1}$  and  $0.05 \text{ h}^{-1}$ . Obviously, under similar conditions and for the tube diameters considered,  $\theta$  is mostly independent of tube diameter, as assumed (see Equation 9).

The light/dark cycle frequency  $\nu$  is a function of the fractional illuminated volume  $\phi$  and the time  $t_d$ . The fractional volume  $\phi$  depends on the light profiles that are influenced by the tube diameter, the dilution rate, the external irradiance level, and the pigment content of the biomass. The time  $t_d$  depends on the light profiles, the tube diameter and the linear velocity  $U_L$ . Therefore, the cycle frequency  $\nu$  implicitly combines the four independent variables considered in this study as affecting the biomass productivity: the dilution rate,  $D$ ; the tube diameter,  $d_t$ ; the day-averaged

Table 1. Variation of the mean biomass concentration,  $C_b$ , with the imposed dilution rate,  $D$ , and culture velocity,  $U_L$ , for photobioreactor with a tube diameter of 0.03 m. Values are shown for the measured average daily irradiance,  $I_{wm}$ ; the calculated illuminated fraction of the reactor,  $\phi$ ; the radial velocity,  $U_R$ ; the angle  $\theta$ ; the dark period,  $t_d$ ; the cycling time,  $t_c$ ; and the light/dark frequency,  $\nu$

Exp. No.	$U_L$ , m s <sup>-1</sup>	$D$ , h <sup>-1</sup>	$I_{wm}$ , $\mu\text{E m}^{-2} \text{s}^{-1}$	$C_b$ , g L <sup>-1</sup>	$P_b$ g L <sup>-1</sup> d <sup>-1</sup>	$\phi$ , %	$U_R$ , m s <sup>-1</sup>	$\theta$ , radians	$t_d$ , s	$t_c$ , s	$\nu$ , Hz
1	0.300	0.025	914	4.30	1.08	3.30	0.020	3.090	0.625	0.646	1.547
2	0.300	0.025	1348	4.90	1.23	9.71	0.020	2.989	0.603	0.668	1.497
3	0.300	0.025	1502	5.90	1.49	9.34	0.020	2.995	0.604	0.667	1.500
4	0.300	0.025	1545	6.80	1.71	10.04	0.020	2.984	0.602	0.669	1.494
5	0.300	0.025	2046	9.10	2.29	10.40	0.020	2.978	0.601	0.670	1.491
6	0.300	0.025	2290	7.50	1.89	12.48	0.020	2.945	0.593	0.678	1.475
7	0.300	0.040	1028	3.30	1.32	18.91	0.020	2.842	0.570	0.702	1.424
8	0.300	0.040	1208	4.20	1.68	21.05	0.020	2.808	0.561	0.711	1.406
9	0.300	0.040	1704	4.90	1.96	29.98	0.020	2.662	0.525	0.750	1.333
10	0.300	0.040	1813	6.00	2.40	28.54	0.020	2.685	0.531	0.743	1.345
11	0.300	0.040	2160	6.00	2.40	26.94	0.020	2.712	0.538	0.736	1.358
12	0.306	0.035	2104	5.86	2.05	30.57	0.020	2.652	0.514	0.740	1.351
13	0.241	0.035	2026	5.81	2.03	30.57	0.016	2.652	0.633	0.911	1.097
14	0.364	0.035	2136	5.84	2.04	32.21	0.023	2.624	0.435	0.642	1.557
15	0.300	0.040	2319	6.10	2.44	32.41	0.020	2.621	0.515	0.762	1.313
16	0.300	0.050	1220	3.40	1.70	29.12	0.020	2.676	0.529	0.746	1.340
17	0.350	0.050	1126	3.41	1.71	17.42	0.023	2.866	0.503	0.609	1.643
18	0.500	0.050	1289	3.82	1.91	31.63	0.031	2.634	0.331	0.485	2.063
19	0.300	0.050	2048	3.60	1.80	52.10	0.020	2.270	0.421	0.880	1.137
20	0.300	0.050	2170	4.30	2.15	61.18	0.020	2.089	0.371	0.956	1.046

incident irradiance,  $I_{wm}$ ; and the liquid velocity,  $U_L$ . An analysis of variance showed that the most important independent variables affecting the light/dark cycle frequency are the tube diameter, the culture velocity, and the dilution rate, in the listed order. The influence of the day-averaged incident irradiance on the cycle frequency is not significant.

The biomass productivity ( $P_b$ ) data are shown in Figure 2 as a function of the light/dark cycle frequency,  $\nu$ . Although the data are somewhat scattered, a significant biomass productivity is achieved only for cycle frequencies of 1 Hz and greater. The scatter in Figure 2 suggests that in addition to frequency, another variable is influencing the behavior. This variable is the day-averaged irradiance,  $I_{wm}$ . An analysis of variance of the productivity data showed that the biomass productivity depended mainly on frequency  $\nu$ , and the day-averaged irradiance,  $I_{wm}$ . The other variables did not directly influence the productivity, although, as explained previously, they did affect the light/dark cycle frequency, hence, having an indirect influence on productivity. Whereas the biomass productivity

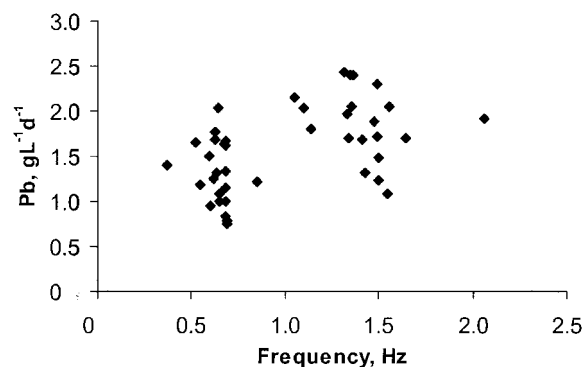


Figure 2. Biomass productivity as a function of light/dark cycle frequency for two values of tube diameter, three values of dilution rate, four values of culture velocity, and several day-averaged irradiances.

increased linearly with increasing day-averaged irradiance value, the variation with the frequency was roughly hyperbolic (Figure 3), according to a Monod type growth equation:

$$P_b = \frac{P_{b \max} \nu}{K_\nu + \nu} \quad (21)$$

Table 2. Variation of the mean biomass concentration,  $C_b$ , with the imposed dilution rate,  $D$ , and the culture velocity,  $U_L$ , for photobioreactor with a tube diameter of 0.06 m. Values are shown for the measured average daily irradiance,  $I_{wm}$ ; the calculated illuminated fraction of the reactor,  $\phi$ ; the radial velocity,  $U_R$ ; the angle  $\theta$ ; the dark period,  $t_d$ ; the cycling time,  $t_c$ ; and the light/dark frequency,  $\nu$

Exp. No.	$U_L$ , m s <sup>-1</sup>	$D$ , h <sup>-1</sup>	$I_{wm}$ , $\mu\text{E m}^{-2} \text{s}^{-1}$	$C_b$ , g L <sup>-1</sup>	$P_b$ , g L <sup>-1</sup> d <sup>-1</sup>	$\phi$ , %	$U_R$ , m s <sup>-1</sup>	$\theta$ , radians	$t_d$ , s	$t_c$ , s	$\nu$ , Hz
21	0.300	0.025	914	3.00	0.76	7.93	0.018	3.071	1.329	1.443	0.693
22	0.300	0.025	1351	3.10	0.78	9.04	0.018	2.999	1.321	1.452	0.689
23	0.300	0.025	1503	3.30	0.83	10.44	0.018	2.977	1.310	1.463	0.684
24	0.300	0.025	1563	4.00	1.01	10.44	0.018	2.977	1.310	1.463	0.684
25	0.300	0.025	1645	5.30	1.34	14.06	0.018	2.920	1.282	1.491	0.680
26	0.300	0.025	2291	6.40	1.61	10.44	0.018	2.977	1.310	1.463	0.684
27	0.300	0.025	2362	6.50	1.64	13.36	0.018	2.931	1.287	1.486	0.673
28	0.300	0.025	2366	6.60	1.66	10.44	0.018	2.977	1.310	1.463	0.684
29	0.300	0.040	1032	2.50	1.00	19.32	0.018	2.836	1.239	1.536	0.651
30	0.300	0.040	1211	2.70	1.08	20.29	0.018	2.820	1.231	1.544	0.648
31	0.300	0.040	1542	3.30	1.32	23.34	0.018	2.771	1.205	1.572	0.636
32	0.300	0.040	1806	4.20	1.68	27.36	0.018	2.705	1.169	1.610	0.621
33	0.300	0.040	2319	4.40	1.76	25.57	0.018	2.734	1.185	1.593	0.628
34	0.300	0.040	2860	5.10	2.04	25.57	0.018	2.734	1.185	1.593	0.638
35	0.300	0.050	1225	2.50	1.25	28.91	0.018	2.679	1.155	1.625	0.615
36	0.350	0.050	1126	1.91	0.96	51.30	0.021	2.285	0.811	1.665	0.601
37	0.350	0.050	1126	2.29	1.15	33.30	0.021	2.606	0.974	1.460	0.685
38	0.500	0.050	1289	2.45	1.23	47.20	0.028	2.362	0.623	1.179	0.848
39	0.500	0.050	1289	2.38	1.19	83.20	0.028	1.527	0.306	1.824	0.548
40	0.300	0.050	2051	3.00	1.50	35.26	0.018	2.573	1.096	1.693	0.591
41	0.300	0.050	2161	3.30	1.65	52.43	0.018	2.264	0.915	1.924	0.520
42	0.300	0.050	2538	2.80	1.40	92.50	0.018	1.147	0.285	3.796	0.366

where  $P_{b\max}$  and  $K_\nu$  are, respectively, the maximum biomass productivity and the frequency at which the productivity is the half of the maximum value. To clarify the influence of  $\nu$  and  $I_{wm}$ , the biomass productivity data were grouped into four sets corresponding to different day-averaged irradiances and a separate fit (Figure 4) was obtained for each set of data according to Equation (21). As is obvious from Figure 4, the day-averaged irradiance strongly affects the parameters in Equation (21). Independent of the  $I_{wm}$  value, there is a frequency threshold of 1–1.5 Hz above which the productivity is not affected (Figure 4).

The Equation (21) parameter values for the four curves in Figure 4 are summarized in Table 3. The  $K_\nu$  values in Table 3 decline as the irradiance values increase. This supports the premise that scale-up using a constant cycle frequency is indeed a suitable criterion; however, if the irradiance level is increased the biomass concentration and productivity increase. Both  $P_{b\max}$  and  $K_\nu$  show a linear dependence on  $I_{wm}$ ;

Table 3. Coefficients of least square fit of Equation (21) for the four curves in Figure 4. Values of  $P_b$  grouped in four sets according to irradiances

$I_{wm}$ , $\mu\text{E m}^{-2} \text{s}^{-1}$	$P_{b\max}$ , g L <sup>-1</sup> d <sup>-1</sup>	$K_\nu$ , Hz
975	1.6	0.59
1225	2.1	0.50
1625	2.3	0.37
2250	2.7	0.35

$P_{b\max}$  increases while  $K_\nu$  declines as the  $I_{wm}$  value increases. The specific relationships are:

$$P_{b\max} = a + bI_{wm} \quad (22)$$

and

$$K_\nu = c + dI_{wm}. \quad (23)$$

Substituting Equation (22) and Equation (23) in Equation (21), we obtain:

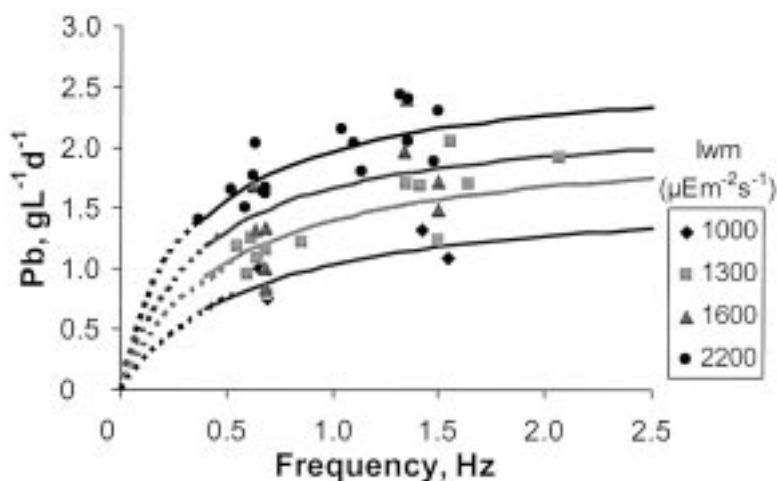


Figure 4. Biomass productivity as a function of the frequency and day-averaged irradiance,  $I_{wm}$ . The 42 experiments in Tables 1 and 2 have been grouped in four sets according to  $I_{wm}$  values.

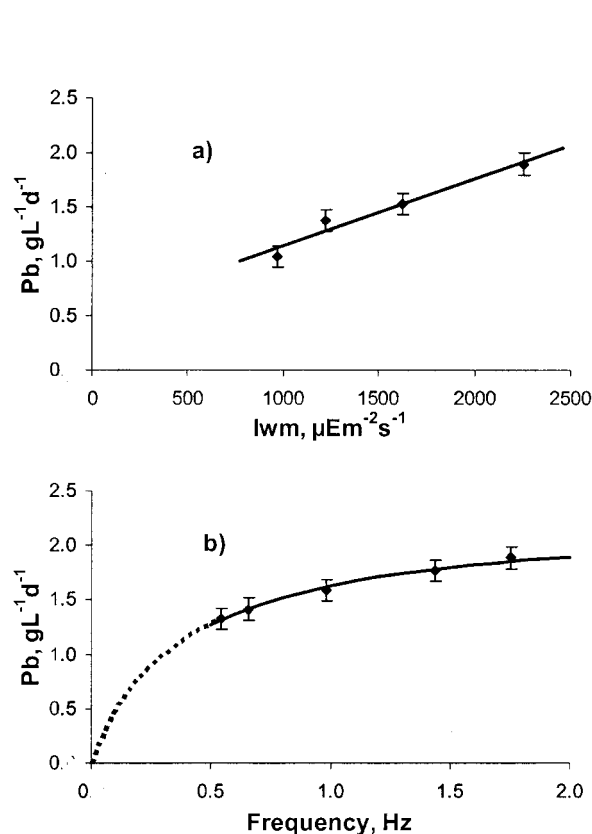


Figure 3. Variation of biomass productivity with (a) the day-averaged irradiance  $I_{wm}$ , and (b) the light/dark cycle frequency. Data from the analysis of variance of the overall experimental results. The error bars represent one standard deviation around the mean.

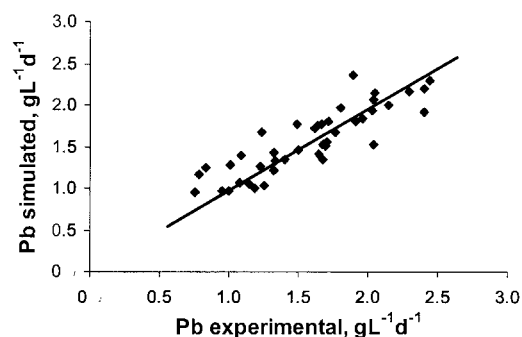


Figure 5. Comparison of predicted and experimental biomass productivity ( $P_b$ ) values. Predicted values were calculated using Equation (24). The straight line represents exact agreement.

$$P_b = \frac{(a + bI_{wm})\nu}{(c + dI_{wm}) + \nu}. \quad (24)$$

Using Equation (24) to fit all the experimental data, the values of the various characteristic parameters are:  $a = 1.42 \text{ g L}^{-1} \text{ d}^{-1}$ ;  $b = 8.8 \times 10^{-4} \text{ g m}^2 \text{ s } \mu\text{E}^{-1} \text{ L}^{-1} \text{ d}^{-1}$ ;  $c = 1.09 \text{ Hz}$ , and  $d = -1.8 \times 10^{-4} \text{ m}^2 \mu\text{E}^{-1}$ . The regression coefficient for the fit was 0.90. Figure 5 compares the experimental productivity data with values predicted by Equation (24), demonstrating a reasonably good fit.

Note that in Figures 3 and 4, the exact location of the productivity versus frequency curves is uncertain near  $\nu = 0$ ; nevertheless, the productivity does approach a value close to zero at  $\nu = 0$ . In view of the definition of frequency specified in Equation (6), a nil value of  $\nu$  occurs only under two conditions: (i) when the culture is so dilute that a dark zone does

not exist (i.e.  $\phi = 1$ ); and (ii) when the dark time is infinitely long (e.g. during the night). Under the first of these situations, the intrinsic photosynthetic productivity of the cells is of course at the maximum value, but the volumetric productivity of the bioreactor is quite small because the cell concentration is quite low. For example, using the previously published data for *P. tricornutum* (Molina Grima et al., 1996), at an extrapolated dilution rate of  $0.059 \text{ h}^{-1}$  (biomass concentration  $\approx 1 \text{ g L}^{-1}$ ; external irradiance  $\approx 2800 \mu\text{E m}^{-2} \text{ s}^{-1}$ ), the estimated productivity is roughly  $0.5 \text{ g L}^{-1} \text{ d}^{-1}$ , or quite close to the origin in Figures 3 and 4. Also, under effective darkness (i.e. when the light intensity is at or below the compensation irradiance) in batch culture, the culture productivity is zero or a little lower because of respiratory losses. (Only  $\sim 10\%$  of the initial biomass is lost by respiration during the night.)

The behavior observed in Figure 4 has also been reported for *Spirulina* in a flat plate reactor (Qiang & Richmond, 1996). For different irradiances an optimum aeration rate (the main factor influencing the cycle frequency) that maximized the biomass productivity was obtained, although the biomass productivity increased with increasing irradiance level. The behavior in Figure 4 is also consistent with the analysis of Terry (1986), who showed that the rate of photosynthesis in *P. tricornutum* (i.e. photosynthetic production of oxygen) is a function of the light/dark cycle frequency, the intensity of light received, and the proportion of the total cycle period during which the cells are illuminated. In Terry's work, the productivity was no longer influenced by frequency once the frequency value exceeded about 5 Hz at light intensities of  $\sim 1000 \mu\text{E m}^{-2} \text{ s}^{-1}$ . In contrast, in Figure 4, the productivity becomes independent of frequency at much lower frequencies. This is because the light-dark cycle of this study is not exactly the same as that of Terry (1986). In Terry's work, the cultures were dilute and shallow; consequently, during the flash period, all cells were exposed to the same light intensity whereas in the dark the light intensity was zero. In Terry's study the cells experienced a true light-dark cycle, but the nature of light-dark cycling in production photobioreactors is quite different, as previously explained. In the present study, as in any production photobioreactor, a true light-dark cycle does not exist for a great majority of the cells but the cells do move from a light saturated to a light-limited zone. Analysis of the effects of this movement is what really matters in scale-up, as relevant to practical situations.

Although Terry's work is not meaningful in the context of practical biomass production systems, it identifies the light/dark cycle frequency as the main variable affecting the oxygen generation rate, or the rate of photosynthesis. Indeed, the  $K_v$  values in Table 3 are similar to ones reported by Terry (1986) for *P. tricornutum*. Although Terry's  $K_v$  values were nearly independent of light intensity, a close inspection of Table II of that paper (Terry, 1986) reveals that at incident irradiances of approximately  $2000 \mu\text{E m}^{-2} \text{ s}^{-1}$ , the light intensity did influence oxygen production.

Terry defined a 'proportional integration of light intensity,  $\Gamma$ ', and related it with the frequency  $\nu$  as follows:

$$\Gamma = \frac{\Gamma_{\max} \nu}{K_v + \nu}. \quad (25)$$

The value of  $\Gamma$  represented the extent to which photosynthesis progressed from no integration of light (i.e. the oxygen production rate was a function of the local values of the light intensity within the culture) to full integration of light intensity (i.e. the oxygen production rate depended on average light intensity, not local values). A  $\Gamma$  value close to unity implies that the culture is averaging the light intensity and a concomitantly higher photosynthetic efficiency. Productivity is close to maximum when  $\Gamma$  equals 1. Thus, the observed productivity may be related to maximum productivity through  $\Gamma$ :

$$P_b = \Gamma P_{b \max}. \quad (26)$$

By substituting Equation (25) in Equation (26), and taking into account Equation (23), we obtain:

$$P_b = \frac{\Gamma_{\max} \nu}{(c + dI_{wm}) + \nu} P_{b \max}. \quad (27)$$

Equation (27) may be used to explain the experimental data. An identical  $\Gamma$  value in two different reactors is a necessary and sufficient conditions for attaining identical productivities in both reactors. In addition, for a given tubular reactor and day-averaged irradiance, the productivity will change with operational conditions only if  $\Gamma$  changes. For example, for a specific photobioreactor characterized by its tube diameter  $d_t$ , the productivity will increase with  $U_L$  so long as  $\Gamma$  will. This is confirmed in Table 4 where experiments 16 and 17, performed at different flow velocities, provide the same productivity because the  $\Gamma$  values for the two runs are the same. Further, the experiment 18 (Table 4) had a 12% higher productivity that was consistent with a similar increase in  $\Gamma$  value.

Table 4. Influence of the culture velocity on the scale-up of tubular photobioreactors. Variation of  $\nu$ , the light integration function,  $\Gamma$ , and the experimental biomass productivity. Values of the tube diameter and dilution rate were 0.03 m and 0.050 h<sup>-1</sup>, respectively

No.	$U_L$ , m s <sup>-1</sup>	$I_{wm}$ , $\mu\text{E m}^{-2} \text{s}^{-1}$	$C_b$ , g L <sup>-1</sup>	$P_b$ , g L <sup>-1</sup> d <sup>-1</sup>	$\nu$ , Hz	$\Gamma$	$P_{b \text{ exp}}/P_{b \text{ max}}$
16	0.30	1220	3.40	1.70	1.340	0.628	0.682
17	0.35	1126	3.41	1.71	1.643	0.674	0.707
18	0.50	1289	3.82	1.91	2.063	0.722	0.748

The agreement between the  $\Gamma$  values (calculated as a function of  $\nu$  and  $I_{wm}$ ) and the experimental ratio of actual productivity to its maximum value, is generally good for the data in Table 4.

Table 5 shows the values of  $\Gamma$  for the experiments 8 and 16 ( $\nu$  values of 1.41 and 1.34 Hz, respectively), performed with the smallest reactor and the lowest reasonable liquid velocity, and experiments 38 and 39 performed with the larger reactor and the maximum attainable liquid velocity. The latter two experiments in the larger reactor were about 40% less productive than experiment 16 (Table 5) performed in the smaller reactor at the same dilution rate. Based on the theory developed here and using the  $\Gamma$  values of 0.41 and 0.52 (Table 5), the predicted average decrease in productivity is 38% for the two experiments. Similarly, Table 6 shows the productivity for eight experiments carried out at the same culture velocity but using different photobioreactors and dilution rates. The ratio between the experimental productivity, for the experiments at the same dilution rate, can be predicted using the developed theory. For example, the ratio between the productivity obtained in experiments 1 and 21 (dilution rate of 0.025 h<sup>-1</sup> and identical  $I_{wm}$  values) is 1.43; the ratio between the respective functions of light integration (i.e.  $\Gamma$  values) for these experiments is 1.41. For the experiments at a dilution rate of 0.04 h<sup>-1</sup> the deviation of the experimental productivity relative to that predicted using the  $\Gamma$  values, is 4%. For the experiments at a dilution rate of 0.05 h<sup>-1</sup>, the experimental and predicted productivities agree almost exactly.

Clearly, our findings verify the premise that light/dark cycling frequency exerts a significant effect on productivity and strengthen the original hypothesis that the light/dark cycle frequency is the most important variable affecting scale-up of photobioreactors. If in a small scale photobioreactor the cycle frequency was greater than 1–1.5 Hz, on scale-up the liquid ve-

locity will need to increase only just enough to attain the noted threshold frequency to obtain the maximum possible productivity. (Increases beyond the threshold limit do not affect productivity.)

### Maximum scaleable tube diameter

Equation (18) allows the calculation of the culture velocity as a function of the scale factor  $f$ , the fractional illuminated volume of the reactor  $\phi$ , and the flow velocity in the small scale reactor  $U_{LS}$ . As noted earlier,  $\phi$  values are nearly identical for the small and the large scale for otherwise similar operational conditions characterized by the same dilution rate ( $D$ ), linear flow velocity ( $U_L$ ), and irradiance ( $I_{wm}$ ). (See for example the data for eight experiments in Table 6). Consequently, Equation (18) can be further simplified because the term  $\alpha^{8/7}$  is about 1; Equation (18) becomes:

$$U_{LL} = f^{9/7} U_{LS}. \quad (28)$$

Figure 6 shows the linear liquid velocity in the larger reactor as a function of the tube diameter for  $f$  values in the range of 0.8–12.8. Some of the noted culture velocities are not practicable because of possible shear damage to cells (Contreras et al., 1998; Chisti, 1999) and limited strength of plastics used in making photobioreactors (Sánchez Mirón et al., 1999). As previously observed for *P. tricornutum* (Contreras et al., 1998), values of shear rates greater than 7000 s<sup>-1</sup>, or microeddies smaller than 45  $\mu\text{m}$  affect the culture. Calculated microeddy lengths for various culture velocities are also noted in Figure 6. The length of the microeddies was calculated (Hinze, 1975) using the equation:

$$l_{\text{eddies}} = \left(\frac{\mu}{\rho}\right)^{3/4} \xi^{-1/4}, \quad (29)$$

Table 5. Influence of the culture velocity and the tube diameter on the scale-up of tubular photobioreactors. Variation of  $\nu$ ,  $\Gamma$ , and biomass productivity

No.	$U_L$ , $\text{m s}^{-1}$	$d_t$ , m	$D$ , $\text{h}^{-1}$	$I_{wm}$ , $\mu\text{E m}^{-2} \text{s}^{-1}$	$P_b$ , $\text{g L}^{-1} \text{d}^{-1}$	$\nu$ , Hz	$\Gamma$	$P_{b \text{ exp}}/P_{b \text{ max}}$
8	0.30	0.025	0.04	1208	1.68	1.406	0.639	0.677
16	0.30	0.025	0.05	1220	1.70	1.340	0.628	0.682
39	0.50	0.050	0.05	1289	1.19	0.548	0.408	0.466
38	0.50	0.050	0.05	1289	1.22	0.848	0.516	0.480

Table 6. Influence of tube diameter and dilution rate on the scale-up of tubular photobioreactors. Culture velocity was  $0.30 \text{ m s}^{-1}$ . Variation of  $\nu$ ,  $\Gamma$ , biomass productivity and illuminated fraction of reactor,  $\phi$

No.	$d_t$ , m	$D$ , $\text{h}^{-1}$	$I_{wm}$ , $\mu\text{E m}^{-2} \text{s}^{-1}$	$P_b$ , $\text{g L}^{-1} \text{d}^{-1}$	$\phi$ , %	$\nu$ , Hz	$\Gamma$	$P_{b \text{ exp}}/P_{b \text{ max}}$
1	0.025	0.025	914	1.08	3.3	1.547	0.661	0.487
7	0.025	0.040	1028	1.32	18.9	1.424	0.642	0.568
8	0.025	0.040	1208	1.68	21.1	1.406	0.639	0.677
16	0.025	0.050	1220	1.70	29.1	1.340	0.628	0.682
21	0.050	0.025	914	0.76	7.9	0.693	0.466	0.340
29	0.050	0.040	1032	1.00	19.3	0.651	0.450	0.430
30	0.050	0.040	1211	1.08	20.3	0.648	0.449	0.434
35	0.050	0.050	1225	1.25	28.9	0.615	0.436	0.500

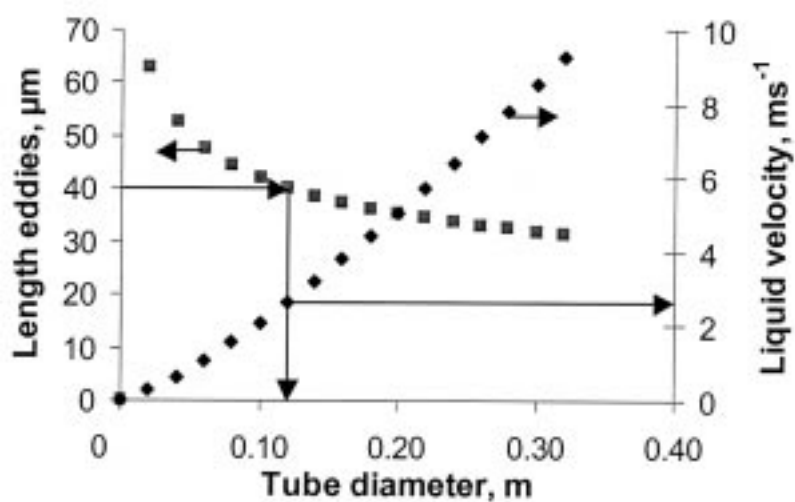


Figure 6. Maximum scaleable tube diameter ( $d_t$ ) for culturing *P. tricornutum*. Variation of the axial culture velocity ( $U_L$ ) and length of microeddies ( $l_{\text{eddies}}$ ) are shown as functions of tube diameter. Eddies smaller than about  $45 \mu\text{m}$  potentially damage cells; thus,  $45 \mu\text{m}$  value limits the tube diameter to around  $0.10 \text{ m}$ .

where  $\xi$ , the energy dissipation per unit mass, was obtained using Equation (16). As shown in Figure 6, the microeddy diameter declines to less than  $45 \mu\text{m}$  when the tube diameter is about  $0.10 \text{ m}$  and the liquid velocity is around  $2 \text{ m s}^{-1}$ . Therefore the maximum tube diameter for culturing *P. tricornutum* at large scale is roughly  $0.10 \text{ m}$ .

## Conclusions

A method is developed for scale-up of tubular photobioreactors. For identical culture performance, the scale-up criterion requires maintaining a constant light/dark cycle frequency at different scales. For the microalga tested, cycle frequencies of  $1.0\text{--}1.5 \text{ Hz}$  provide an optimal productivity for given conditions of the day-averaged irradiance. The  $\sim 1 \text{ Hz}$  frequency value applies under outdoor conditions of intense sunlight, irrespective of the diameter of the photobioreactor tube. Increasing flow velocity to obtain greater values of cycle frequency is not beneficial and may be detrimental because of shear damaging effects (Contreras et al., 1998; Chisti, 1999). The noted optimal light/dark cycle frequencies are for the alga *P. tricornutum*, but similar values are expected for most other microalgae. For the microalga used, tube diameters larger than about  $0.10 \text{ m}$  would require an unrealistically high culture velocity of  $> 2 \text{ m s}^{-1}$ . Although the latter value is potentially damaging to cells (Sánchez Mirón et al., 1999), it can be attained with airlift pumps (Chisti, 1989) that are about  $8 \text{ m}$  tall. Further work is needed on the effects of light/dark cycle frequencies, especially in the range of  $0$  to  $1 \text{ Hz}$ , and in photobioreactors that are relevant to mass culture.

## Acknowledgements

This research was supported by the European Union (contract BRPR CT97 0537) and Junta de Andalucía, Plan Andaluz de Investigación II (CVI 173).

## References

Acién Fernández FG, García Camacho F, Sánchez Pérez JA, Fernández Sevilla JM, Molina Grima E (1997) A model for light distribution and average solar irradiance inside outdoor tubular photobioreactors for the microalgal mass culture. *Biotechnol. Bioengng* 55: 701–714.

- Acién Fernández FG, García Camacho F, Sánchez Pérez JA, Fernández Sevilla JM, Molina Grima E (1998) Modelling of biomass productivity in tubular photobioreactors for microalgal cultures: Effects of dilution rate, tube diameter and solar irradiance. *Biotechnol. Bioengng* 58: 605–616.
- Chisti Y (1989) *Airlift Bioreactors*. Elsevier, London, 203–219.
- Chisti Y (1999) Shear sensitivity. In Flickinger MC, Drew SW (eds), *Encyclopedia of Bioprocess Technology: Fermentation, Biocatalysis, and Bioseparation*, Vol. 5. Wiley, New York, 2379–2406.
- Contreras Gomez A, Garcia Camacho F, Molina Grima E, Merchuk JC (1998) Interaction between  $\text{CO}_2$ -mass transfer, light availability, and hydrodynamic stress in the growth of *Phaeodactylum tricornutum* in a concentric tube airlift photobioreactor. *Biotechnol. Bioengng* 60: 317–325.
- Davies JT (1972) *Turbulence Phenomena*. Academic Press, London, 27–28.
- García Camacho F, Contreras Gómez A, Acién Fernández FG, Fernández Sevilla JM, Molina Grima E (1999) Use of concentric tube airlift photobioreactors for microalgal outdoor mass cultures. *Enzyme Microb. Technol.* 24: 164–172.
- Grobbelaar JU (1994) Turbulence in algal mass cultures and the role of light/dark fluctuations. *J. appl. Phycol.* 6: 331–335.
- Grobbelaar JU, Nedbal L, Tichý V (1996) Influence of high frequency light/dark fluctuations on photosynthetic characteristics of microalgae photoacclimated to different light intensities and implications for mass algal cultivation. *J. appl. Phycol.* 8: 335–343.
- Hansmann E (1973) Pigment analysis. In Stein JR (ed.), *Handbook of Phycological Methods, Culture Methods and Growth Measurements*. Cambridge University Press, London, 359–368.
- Hinze JO (1975) *Turbulence*, McGraw Hill, New York.
- Janssen M, Kuijpers TC, Veldhoen B, Ternbach MB, Tramper J, Mur LR, Wijffels RH (1999) Specific growth rate of *Chlamydomonas reinhardtii* and *Chlorella sorokiniana* under medium duration light/dark cycles: 13–87 s. *J. Biotechnol.* 70: 323–334.
- Kok B (1953) Experiments on photosynthesis by *Chlorella* in flashing light. In Burlew JS (ed.), *Algal Cultures from Laboratory to Pilot Plant*. Publication 600. Carnegie Institution of Washington, Washington D.C., 63–158.
- Kroon BMA (1994) Variability of photosystem II quantum yield and related processes in *Chlorella pyrenoidosa* (Chlorophyta) acclimated to an oscillating light regime simulating a mixed photic zone. *J. Phycol.* 30: 841–852.
- Mann JE, Myers J (1968) On pigments, growth and photosynthesis of *Phaeodactylum tricornutum*. *J. Phycol.* 4: 349–355.
- Matthijs HCP, Balke H, Hes van UM, Kroon BMA, Mur LR, Binot RA (1996) Application of light-emitting diodes in bioreactor: flashing light effect and energy economy in algal culture (*Chlorella pyrenoidosa*). *Biotechnol. Bioeng.* 50: 98–107.
- Merchuk JC, Ronen M, Giris S, Arad S (1998) Light/dark cycles in the growth of the red microalga *Porphyridium* sp. *Biotechnol. Bioengng* 59: 705–713.
- Molina Grima E, Acién Fernández FG, Garcia Camacho F, Chisti Y (1999) Photobioreactors: light regime, mass transfer, and scale-up. *J. Biotechnol.* 70: 231–248.
- Molina Grima E, Sánchez Pérez JA, García Camacho F, Fernández Sevilla JM, Acién Fernández FG (1996) Productivity analysis of outdoor chemostat culture in tubular airlift photobioreactors. *J. appl. Phycol.* 8: 369–380.
- Nedbal L, Tichý V, Grobbelaar JU, Xiong VF, Neori A (1996) Microscopic green algae and cyanobacteria in high-frequency intermittent light. *J. appl. Phycol.* 8: 325–333.

- Philliphs JN, Myers J (1954) Growth rate of *Chlorella* in flashing light. *Plant Physiol.* 29: 152–161.
- Qiang H, Richmond A (1996) Productivity and photosynthetic efficiency of *Spirulina platensis* as affected by light intensity, algal density and rate of mixing in a flat plate photobioreactor. *J. appl. Phycol.* 8: 139–145.
- Sánchez Mirón AS, Gómez Contreras A, García Camacho FG, Molina Grima E, Chisti Y (1999) Comparative evaluation of compact photobioreactors for large-scale monoculture of microalgae. *J. Biotechnol.* 70: 249–270.
- Terry KL (1986) Photosynthesis in modulated light: Quantitative dependence of photosynthetic enhancement on flashing rate. *Biotechnol. Bioengng* 28: 988–995.
- Whyte JC (1987) Biochemical composition and energy content of six species of phytoplankton used in mariculture of bivalves. *Aquaculture* 60: 231–241.
- Yongmanitchai W, Ward O (1991) Growth of and omega-3 fatty acid production by *Phaeodactylum tricorutum* under different culture conditions. *Appl. envir. Microbiol.* 2: 419–425.